FERTILITY PRESERVATION

CrossMark

Xenotransplantation of pre-pubertal ovarian cortex and prevention of follicle depletion with anti-Müllerian hormone (AMH)

Laura Detti [1,2,3] · Nicole M. Fletcher [4] · Ghassan M. Saed [4] · Trevor W. Sweatman [5] · Rebecca A. Uhlmann [4] · Alberto Pappo [6] · Irene Peregrin-Alvarez [1]

Abstract

Objective To determine whether recombinant AMH (rAMH) could prevent post-transplant follicular depletion by acting on the stemness markers Oct-4, Sox2, and NANOG.

Materials and methods This was an experimental study where 12 ovariectomized nude mice were xenotransplanted with vitrified/warmed ovarian cortex obtained from a pre-pubertal girl and Alzet pumps delivering rAMH, or placebo (control), were inserted intra-abdominally. Previously vitrified/warmed ovarian cortex fragments were transplanted after 7 days and then harvested after 14 days from pump placement. We performed real-time RT-PCR analyses, ELISA for AMH, FSH, and estradiol, histologic measurement of ovarian follicles, and immunohistochemistry for Ki67 and TUNEL. The main outcome measures were serum levels and tissue expression of the parameters under investigation and follicle count.

Results Serum AMH, FSH, and estradiol reflected post-ovariectomy profiles and were mildly influenced by rAMH administration. Ovarian cortex expression of AMH, AMH-R2, VEGF, GDF9, Oct-4, and Sox2 was lower in rAMH mice than in controls, while NANOG was upregulated. There was a non-significant decrease in primordial follicles after vitrification-warming, and xenotransplantation further decreased this number. There were lower cell replication and depressed apoptosis in the rAMH group.

Conclusions Administration of recombinant AMH in the peri-transplant period did not protect the initial follicular depletion but decreased apoptosis and cellular activation and regulated stem cell markers' tissue expression. These results aid our understanding of the inhibitory effects of AMH on follicular development and show the benefit of administering exogenous AMH at the time of pre-pubertal ovarian cortex transplant to protect the follicles from pre-activation and premature depletion.

Keywords Pre-pubertal · Ovarian cortex · Vitrification · Stemness · Xenotransplant · Recombinant AMH

✉ Laura Detti
ldetti@uthsc.edu

1 Department of Obstetrics and Gynecology, University of Tennessee Health Science Center, Memphis, TN, USA

2 Department of Surgery, University of Texas Rio Grande Valley, Edinburg, TX, USA

3 Division of Reproductive Endocrinology and Infertility, Rout Center, 853 Jefferson Ave, Rm E102, Memphis, TN 38163, USA

4 The C. S. Mott Center for Human Growth and Development, Wayne State University School of Medicine, Detroit, MI, USA

5 Department of Pharmacology, University of Tennessee Health Science Center, Memphis, TN, USA

6 St. Jude Children's Research Hospital, Memphis, TN, USA

Introduction

Ovarian tissue preservation techniques have been primarily applied to post-pubertal females undergoing chemotherapy or radiotherapy for different conditions, mainly cancer. Successful transplantation has so far been measured by the achievement of pregnancy and it has been confirmed in at least 130 patients up to 2015, even though the number of transplants necessary to achieve those results remains unknown. However, a 29% pregnancy rate, with a live-birth rate of 23%, was calculated on 111 patients from five major centers in Europe [1]. Fertility is only one of the benefits achieved with autotransplantation of ovarian cortex, which, perhaps more importantly, also includes a return to normal ovarian endocrine function. This return to function is of foremost importance in pre-pubertal girls, who could regain their ability to

🖄 Springer

undergo spontaneous puberty, in addition to preserving their bone, cardiovascular, and overall health [2].

The overall childhood cancer survival rates in the USA have improved to greater than 80% of affected children as of 2014 [3]. This has prompted increased awareness of long-term quality of life concerns, including, but not limited to, primary ovarian insufficiency [4]. In pre-pubertal girls, surgical removal of the ovarian cortex with subsequent auto-transplant would be the procedure of choice, not just for fertility preservation but also to insure a post-cure optimal quality of life. However, the procedure remains experimental and requires approval from the Institutional Review Board, and, in some blood-borne cancers, the technique carries the risk of reseeding the disease. In addition, technical difficulties for tissue harvesting and freezing (slow freezing versus vitrification) preclude the widespread use of this practice in that population [5].

Whichever freezing technique is used, in ovarian cortex transplant studies, there is massive depletion of primordial follicles during the first week after transplant [6]. This phenomenon has been explained with the slow vascularization of the transplanted tissue and hypoxia-driven follicular damage. In transplant studies of previously frozen/warmed tissue, poor vascularization and hypoxia are still the most plausible causes, rather than the cryopreservation process itself [7]. Revascularization of grafts in a human xenograft model seems to depend not only on neo-angiogenesis from the host but also on existing blood vessels in the grafted tissue [8]. In fact, chimeric vessels are present in the xenografted tissue after 7 days from transplant. However, in recent years, a second, more plausible, mechanism of follicular depletion has surfaced, which finds that the premature activation of primordial follicles and their consequent apoptosis is the principal mechanism of follicular depletion [9].

Efforts have been made to prevent follicular depletion after transplant and several attempts have been made at finding *follicular protectants* after ovarian cortex tissue transplantation, with different results. Gonadotropins like follicle-stimulating hormone (FSH) and luteinizing hormone (LH) were found to cause depletion, rather than protection, of primordial follicles [10, 11]. Peri-transplantation administration of the gonadotropin-releasing hormone (GnRH)-agonist triptorelin pamoate did not prevent primordial follicle depletion after xenografting [12]. In fact, triptorelin caused an additional loss of follicles when administered during the critical neo-vascularization period, soon after transplantation. The anti-apoptotic molecule sphyngosine-1-phosphate and the angiogenic factor vascular endothelial growth factor (VEGF) have been reported to improve the immediate post-transplant follicular loss [13–15]. More recently, inhibitors of the mammalian target of rapamycin (mTOR) signaling pathway have been described as promising ovarian cortex protectant [16, 17]. Consistent performance of the various molecules is currently lacking and further studies are needed to validate the results.

Our group has reported on the inhibitory effects of anti-Müllerian hormone (AMH) on freshly explanted, as well as, vitrified–warmed ovarian cortex tissue [18, 19]. In fact, fresh ovarian cortex tissue cultured in the absence of AMH showed upregulation of ovarian cortex tissue AMH production and increased sensitivity to FSH and LH by upregulation of their receptors. When, instead, the tissue was exposed to increasing in vitro concentrations of AMH, there was downregulation of hormone and pituitary hormone receptor expression. These findings confirmed the inhibitory role of AMH and, at least in part, explained how AMH regulates the cyclic selection for dominance of the antral follicles [18]. Exposing vitrified/warmed ovarian cortex tissue to increasing in vitro concentrations of AMH caused downregulation of the oocyte activation marker growth differentiation factor-9 (GDF9) and of stemness markers such as Octamer-binding transcription factor-4 (Oct-4), sex determining region Y (SRY)-box 2 (Sox2), and homeobox protein NANOG (NANOG), while upregulating VEGF [19]. These transcription factors generate direct reprogramming of differentiated somatic cells to create induced pluripotent stem cells that are indistinguishable from embryonic stem cells (=stemness potential). By downregulating the stemness factors, AMH stalled tissue activation, which substantiated the regulatory role of AMH on ovarian tissue regenerative potential. In addition, Kano et al. recently found that AMH-treated mature mice preserved their reservoir of primordial follicles during administration of chemotherapeutic agents such as carboplatin, doxorubicin, or cyclophosphamide [20].

To further support the hypothesis that AMH has a role in preventing post-transplant follicular tissue activation by inhibiting the stemness markers, we designed an in vivo study in which we transplanted pre-pubertal human ovarian cortex to previously ovariectomized nude mice treated with recombinant AMH (rAMH) via infusion pump. We then evaluated the tissue expression of AMH, its receptor, AMH-R2, FSH receptor (FSH-R), VEGF, GDF9, Oct-4, SOX2, and NANOG by real-time RT-PCR, and serum levels of AMH, estradiol, and FSH by ELISA, in addition to performing histologic evaluation for cell replication and apoptosis by immunohistochemistry.

Materials and methods

This was a pilot experimental study. We obtained fresh ovarian cortex from a 13-year-old peripubertal patient who had not reached menarche, yet. The patient and her parents were presented the study and signed an informed consent form prior to being enrolled. She underwent a right oophorectomy for a fibro-thecoma and the normal ovarian cortex tissue was

harvested from the operative specimen. The repository study was approved by the University of Tennessee Health Science Center Human Investigation Committee (UTHSC-HIC) and is currently registered at ClinicalTrials.gov (NCT02431884). Use of the ovarian cortex specimens for the proposed animal study was obtained from the UTHSC-HIC in June 2014, protocol no. 14-03204-XM. In addition, the study was approved by the UTHSC Institutional Animal Care and Use Committee (IACUC) in 2015, protocol no. 14-066.0, which assured animal welfare.

The ovarian cortex harvested from the surgical specimen was prepared and vitrified within 2 h following our established tissue vitrification protocol. Figure 1 shows sections of ovarian cortex soon after explant and after vitrification-warming. One oocyte surrounded by a monolayer of flat, or cubic, granulosa cells enclosed by a basement membrane identified a primordial (PDF) and a primary follicle (PRF), respectively. Secondary follicles (SEFs) were identified with one oocyte surrounded by multiple cubic granulosa cells and tertiary follicles (TEF) by fluid accumulation amid the granulosa cells (however, no TEFs were identified in any of the specimens in our study). Tissue was cut in 10–20 mm (length) × 3–4 mm (width) × 1 mm (depth) stripes. Induction was carried out in a medium-concentration solution of sucrose and ethylene glycol for up to 15 min, until the stripes would descend to the bottom of the tube. The tissue specimens were then passed into a new tube containing a high concentration of the same solutes until they would descend to the bottom of the tube. The stripes were then plunged into liquid nitrogen and stored in a liquid nitrogen cryo-tank until ready to be warmed. The vitrified specimens necessary for this study were warmed after being in liquid nitrogen for 18 months, following our

protocol, and were then treated. The specimens were further dissected to obtain a total of 25 fragments, each measuring approximately 2.0 (length) × 2.0 (width) × 1.0 (depth) mm and were incubated for 2 h at 37 °C in a pH-adjusted gamete buffer media without rAMH. A smaller fragment was flash-frozen soon after incubation (post-thaw), to provide a baseline for our immunohistochemistry and real-time RT-PCR studies. Figure 1b shows a section of ovarian cortex soon after warming.

We used 10-week-old NU/J mice, or nude mice, imported from Jackson Laboratory (athymic nude, nu-nu; BarHarbor, ME 04609) because this strain has a genetic mutation (disruption of the FOXN1 gene) that causes an inhibited immune system. For this reason, it can receive many different types of tissue grafts (xenografts), as it mounts no rejection response. Ovulation starts at 2.5 months and ends early, at 4 months of age. The mice were bred as per Jackson Lab guidelines and maintained in cages in isolation in the Animal Center at UTHSC under a 12-h light/dark cycle with food and water ad libitum.

A timeline of the experiment is reported in Fig. 2. At time 0, all mice underwent a blood draw from the retro-orbital region, bilateral ovariectomy, and osmotic pump intraperitoneal placement through the same sub-umbilical incision (Fig. 1). The osmotic pump (ALZET Osmotic Pumps, model 1002, Cupertino, CA, USA) administered either normal saline (placebo group) or recombinant human AMH (R&D Systems, Inc., Minneapolis, MN, USA; rAMH group) at a daily dose of 1.23 μg, with a flow rate (Q_T) of 0.25 μL/h based on a mouse temperature of 36.9 °C and a tissue osmolality of 7.5 atm. The pump administered a total of 17.2 μg of recombinant human AMH over the 2-week duration of the experiment. The daily

Fig. 1 Ovarian tissue specimens stained with hematoxylin-eosin showing follicles, indicated by black arrows. **a** Primordial follicles in the fresh tissue, soon after explant. **b** Primordial follicles (PDFs) in rAMH group. **c** Primary follicle (PRF) in the placebo group. **d** Secondary follicle (SEF) in the placebo group
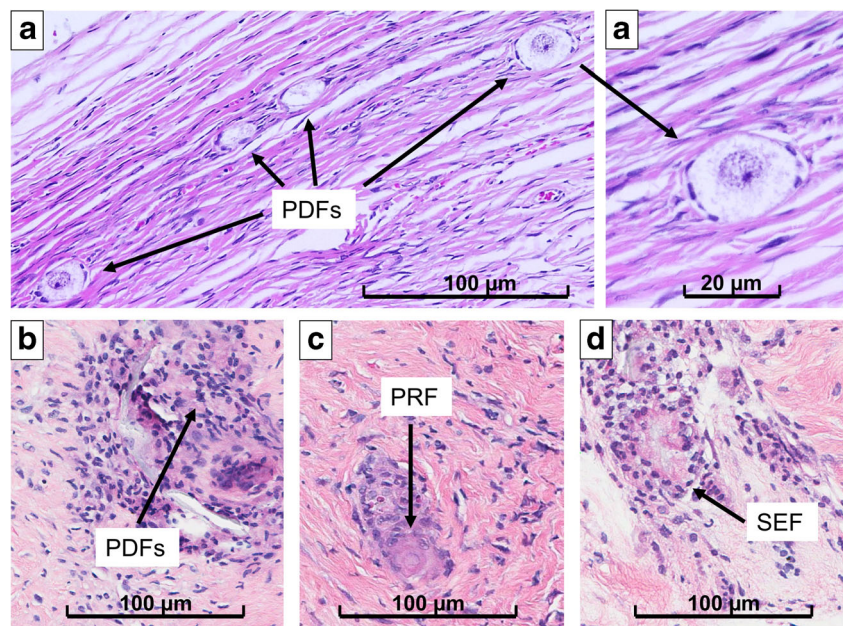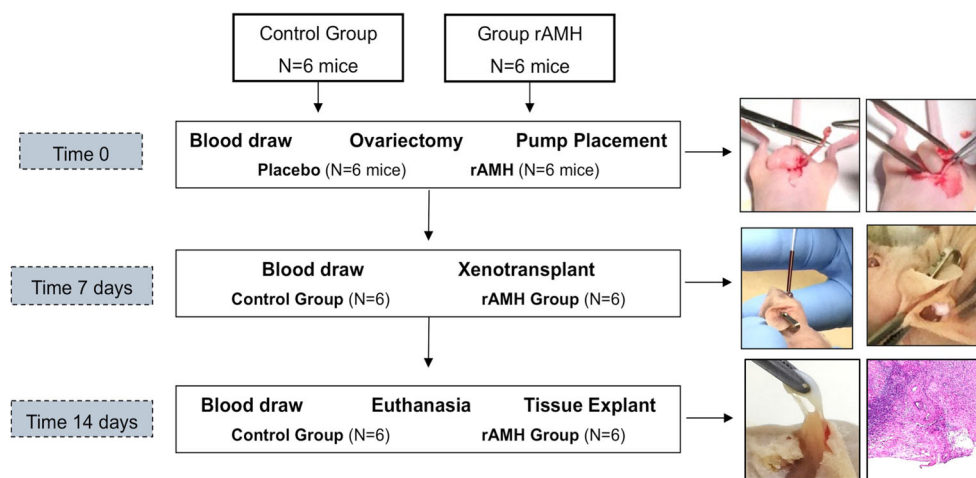
Fig. 2 Timeline of the experiment with pictures showing the procedure performed at each time point. At the bottom are shown the macroscopic and microscopic photographs of an implant's hylum

AMH dose of 1.23 μg was chosen based on previous in vivo work by Parry et al. [21], as well as by our group's previous in vitro study which found a tissue AMH concentration of 0.5 ± 0.1 pg/mL with a serum concentration of 2.0 ng/mL [18]. By doing this, mice were conditioned with either saline or rAMH for 7 days prior to xenotransplant. At time 7 days, all mice underwent a blood draw and were then grafted in the interscapular region with two ovarian cortex fragments measuring approximately $2.0 \times 2.0 \times 1.0$ mm. At time 14 days (on day 14 post-ovariectomy/pump placement and day 7 post-xenotransplantation), all mice were euthanized. This time point was chosen based on the identification of the hypoxic period before day 5 and progressive re-oxygenation from day 5 to day 10 after ovarian cortex transplant [8]. All mice underwent a blood draw just prior to euthanasia and the ovarian cortex fragments were explanted for real-time RT-PCR and histological analyses. The osmotic pumps were recovered to confirm that their content had been completely delivered.

Ovarian tissue processing

After dissection, a portion of the ovarian specimen was fixed in formalin, embedded in paraffin, and stained with hematoxylin and eosin (H&E) and with immune stains. The H&E-stained slides were used to evaluate the follicle number, while the immune-stained slides were used for examination of follicular development. Five-micrometer-thick sections were serially cut and every fifth section analyzed for follicular counts. All ovarian cortex specimens were obtained from each group, and at least four sections were analyzed in each tissue specimen. The computerized program used for image analysis, Spectrum (Version 10.2.2.2314; by Aperio, Vista, CA, USA), allowed us to examine all the sections at the same time and to accurately count all the follicles in each section without redundancy. For follicle counting, the investigators were blinded to the treatment groups.

The rest of the specimen was flash-frozen for PCR analyses, which were executed in triplicates.

Immunohistochemistry

Terminal deoxynucleotidyl transferase (TdT) dUTP Nick-End Labeling (TUNEL) assay is designed to detect apoptotic cells that undergo extensive DNA degradation during the late stages of apoptosis. Staining was performed at room temperature with the DeadEND Colorimetric TUNEL System (Promega, Madison, WI, USA). Tissues on slides were deparaffinized in xylenes (Fisher Scientific, USA), 3×5 min each. Tissues were rehydrated with successive washes in 100, 95, 85, 70, and 50% ethanol for 3 min each. Slides were washed with 0.85% NaCl and then in phosphate-buffered serum (PBS), 5 min each. Tissues were fixed in 4% paraformaldehyde for 15 min and washed in PBS 2×5 min each. Tissue sections were covered with proteinase K (20 μg/mL) for 10 min and then washed for 5 min in PBS. Tissues were re-fixed in 4% paraformaldehyde for 5 min. A positive control was incubated with DNAse I to introduce DNA breaks. Tissues were equilibrated in equilibration buffer for 10 min followed by incubation with the biotinylated nucleotide reaction mixture, per the manufacturer's protocol, for 60 min in a humidified incubator at 37 °C. The reaction was terminated by addition of 2× saline-sodium citrate (SSC) followed by washing in PBS, 2×5 min each. Endogenase peroxidase was blocked by incubation in 0.3% H_2O_2 for 5 min followed by washing in PBS 2×5 min each. 3–3′-Diaminobenzidine (DAB; Genecopoeia, Rockville, MD, USA) solution was added to the slides and incubated for several minutes followed by rinsing in distilled water and mounting in Permount (Fisher Scientific, USA).

Ki-67 is a nuclear non-histone protein that is associated with cellular proliferation. It is present at low levels during cellular growth and interphase but is increased in proliferating cells, especially during DNA synthesis in the mitotic phase. In

addition, it is associated with ribosomal RNA transcription [22]. All staining was performed at room temperature. Tissues on slides were deparaffinized in xylenes (Fisher Scientific, USA), 3 × 5 min each. Tissues were rehydrated with successive washes in 100, 95, 85, 70, and 50% ethanol for 3 min each. Slides were washed with 0.85% NaCl and then in PBS, 5 min each. Tissues were fixed in 4% paraformaldehyde for 15 min and washed in PBS 2 × 5 min each. Antigen unmasking was performed in antigen unmasking solution (1×, Vector Laboratories, Burlingame, CA, USA) 100 °C 10 min. Endogenase peroxidase was blocked by incubation in 3% H_2O_2 for 10 min followed by washing in 0.025% Triton-X in PBS 2 × 2 min each. Tissues were blocked with 2.5% normal goat antibody (ImmPRESS Kit, Vector Laboratories) for 20 min followed by incubation in mouse anti-human Ki67 antibody (DAKO) diluted 1:100 in antibody diluent (DAKO, Fisher Scientific, USA). Slides were washed for 5 min in PBS and then incubated for 30 min in ImmPRESS Reagent (ImmPRESS Kit, Vector Laboratories). Slides were again washed 2 × 5 min each in PBS and incubated for 8 min in DAB solution and rinsed 2× in distilled water. Slides were counterstained with hematoxylin (Genecopoeia, Rockville, MD, USA) for 2 min, rinsed in distilled water, and tissue sections were dehydrated in successive washes of 75, 95, and 100% ethanol, 2 min each. Tissues were cleared with xylenes for 5 min and mounted in Permount.

Real-time RT-PCR analysis

We utilized real-time RT-PCR to determine tissue mRNA levels for GDF9, VEGF, Oct-4, Sox2, and NANOG, in addition to quantifying tissue mRNA levels for AMH itself and its receptor, AMH-R2, in all specimens.

Total RNA was extracted from tissues with the RNeasy Mini Kit (Qiagen). Frozen tissues were first homogenized in lysis buffer provided in the kit and run through a QIA tissue shredder column (Qiagen) followed by RNA extraction according to the protocol provided by the manufacturer. A 20-µL cDNA reaction volume using an equal amount of RNA (up to 1 µg) was prepared using the SuperScript VILO MasterMix Kit (Life Technologies, Grand Island, NY), as described by the manufacturer's protocol. Real-time RT-PCR was performed with the Express SYBR GreenER qPCR SuperMix RT-PCR kit (Life Technologies) and a Cepheid 1.2f Detection System (Cepheid, Sunnyvale, CA). Each 25-µL reaction included 12.5 µL of 2x QuantiTect SYBR Green RT-PCR master mix, cDNA template, and 0.2 µM each of target-specific primer were selected with the aid of the software program, Beacon Designer (Premier Biosoft, Palo Alto, CA). Human oligonucleotide primers that amplify variable portions of the protein coding regions were established and verified, described in Table 1, as previously described [18, 19, 23]. Standards with known concentrations were designed specifically for β-actin (79 base pairs (bp)), AMH (102 bp), AMH-R2 (81 bp), GDF9 (91 bp), NANOG (84 bp), OCT4b (82 bp), SOX2 (153 bp), and VEGF (132 bp) using the Beacon Designer software, allowing for construction of a standard curve using a tenfold dilution series. An individual standard for each gene of interest provides a method for absolute quantification of the gene in interest. The PCR reaction conditions were programmed as follows: an initial cycle was performed at 95 °C for 60 s. Next, there were 35 cycles of denaturation at 95 °C for 15 s, annealing time, and temperatures as described in Table 1, followed by a final cycle at 72 °C for 30 s to allow completion of product synthesis. A melting curve analysis was performed to demonstrate the specificity of the PCR product as a single peak. A control, which contains all the reaction components except for the template, was included in all experiments.

Blood processing

Blood obtained from the retro-orbital region was refrigerated and spun. The serum was isolated, frozen, and kept at − 80 °C until analysis. We measured human AMH, human estradiol, and murine FSH, to evaluate the function of the xenotransplanted ovarian cortex. Detection of human AMH, human estradiol, and murine FSH in serum was performed utilizing the Human Mullerian Inhibiting Substance ELISA (MyBioSource, San Diego, CA), the Estradiol ELISA (Invitrogen), and the FSH ELISA (Enzo Life Sciences, Ann Arbor, MI), all per the manufacturers' protocols. Data was normalized per microliters of serum tested.

Statistical analysis

All our variables were continuous; however, because of the skewed distribution, our results were summarized as median and quartiles (Q_1, Q_3). We compared medians and used the non-parametric Mood's median test to evaluate changes in mRNA and blood serum levels within the groups *post-thaw*, *xenotransplant*, and *euthanasia*. Mood's median test is based on the same assumptions of the chi-square test: we used this rather than the Kruskal-Wallis test because the Mood's test is more robust against outliers and some extreme values were observed in the data.

For blood serum levels, we used the same test to evaluate the changes between the placebo and rAMH groups of mice at the various time points. We used SPSS v24 for Windows (SPSS, Chicago, IL); a $p < 0.05$ defined significance.

Results

All mice survived the two surgical procedures and did not develop infections or any adverse outcomes. All of them were

Table 1 Real-time RT-PCR oligonucleotide primer sequences and cycling conditions

Accession no.	Gene	Sense (3′-5′)	Antisense (5′-3′)	Amplicon length (bp)	Annealing temperature (°C)	Annealing time (s)
NM_001101	β-actin	ATGACTTAGTTGCGTTACAC	AATAAAGCCATGCC AATCTC	79	58	10
NM_000479	AMH	GTGCTGCTGCTGAAGATG	CTCCGACAGGCTGATGAG	102	62	10
NM_001164690	AMH-R2	CCAGAAGCACGGCTGACAG	TGGAAAGGGGTGGCTCTCT	81	62	10
NM_001288824	GDF9	TCGCATTACTACCGTTGAA	CACACATTTGACAGCAGAG	91	53	10
NM_024865	NANOG	ACTCTCCAACATCCTGAA	TTCTGCCACCTCTTAGAT	84	55	30
NM_203289	OCT4b	AGGCACTTCTACAGACTATT	CACACCAGTTATCAATCTCC	82	58	30
NM_003106	SOX2	GGATGGTTGTCTATTAACTT	TCAAACTTCTCTCCCTTT	153	53	30
NM_003376	VEGF	GGAAACCAGCAGAA AGAGG	AAGCAGGTCACTCACTTTG	132	59	10

sacrificed 14 days after undergoing ovariectomy and intra-abdominal pump placement and 7 days after undergoing xenotransplant of human ovarian cortex. All ovarian cortex tissue specimens developed neo-vascularization within 1 week from xenotransplant (Fig. 2, bottom pictures). The tissue specimens did not show ubiquitous neo-vascularization, which would keep them adherent to the surrounding muscle and subcutaneous tissue, but, rather, developed a single hilum with arterial and venous vessels that originated from the underlying muscle in all cases. There was no vasculature between the ovarian cortex specimen and the overlying subcutaneous tissue. All the recovered osmotic pumps were found to be empty of their contents and were still free-floating inside the peritoneal cavity. Figure 1 shows sections of ovarian cortex from the different groups. The fresh cortex was comprised almost exclusively of PDFs (312.5/mm^3; 309.3, 315.4) with rare PRF (21.2/mm^3; 21.0, 22.2). There were no SEF, or TEF, follicles in the fresh tissue. The matrix appeared heterogeneous after vitrification-warming (Fig. 1b), and the follicles were slightly distorted. In the post-warming specimens, there were fewer PDFs than in fresh specimens (279.1/mm^3; 277.8, 292.1; $p = 0.061$). PDFs further decreased after xenotransplantation ($p = 0.013$); however, in the rAMH group, the PDF number was not different from the placebo group, as reported in Table 2. No PRF or SEF follicles were in the post-warming, or rAMH group, whereas the placebo group counted 70.3/mm^3 (57.3, 80.1, PRFs) and 14.1/mm^3 (7.0, 29.2, SEFs) (Table 2). No tertiary follicles were identified in any of the specimens.

Blood serum test results

Table 3 reports the serum concentration for human AMH, human estradiol, and murine FSH in the two mice groups, placebo and rAMH, during the three time points of the experiment. Serum concentration of AMH was maximum on day 0, at time of ovariectomy, and it was minimum at time 14 days, when euthanasia was performed (Fig. 3). The differences across group medians were significant, with $p = 0.05$ in the placebo and $p = 0.011$ in the rAMH group, respectively. At time 14 days, the rAMH group showed significantly higher serum AMH than the placebo group ($p = 0.029$). The decrement at time 14 days was more prominent in the placebo group. However, the PCR results showed a significantly higher ovarian cortex expression of AMH, indicating that tissue production was more important in the placebo group than in the rAMH group (Table 4). The fact that we were able to measure AMH at time 0 showed that human and mouse AMH could equally bind to the human AMH assay used in our experiment, and hence we lost resolution in distinguishing the AMH produced by the xenotransplanted ovarian cortex from the mouse-produced AMH. This prevented us from building an elimination half-life curve for human AMH in the mouse; however, in the placebo group, we calculated a decrement in serum murine AMH of 36.4% (3.032 ng/mL) in 7 days. Dividing 3.032 by 7 days, we found that 0.433 ng/mL (5.2%) AMH was cleared from the bloodstream every day by the mouse. Serum estradiol measurements reflected the physiologic response to ovariectomy and exposed the assay's

Table 2 Ovarian cortex concentration of primordial (PDF), primary (PRF), and secondary follicles (SEF) in the post-warming tissue and the two mice groups, placebo and rAMH

Variable	Post-warming Median (Q1, Q3)	Placebo group Median (Q1, Q3)	rAMH group Median (Q1, Q3)	p value[a]
PDF/mm^3	279.1 (270.0, 279.4)	126.5 (97.0, 129.8)	113.3 (94.8, 223.0)	0.786
PRF/mm^3	0	70.3 (57.3, 80.1)	0	0.036
SEF/mm^3	0	14.1 (7.0, 18.1)	0	0.143

[a] Mood's test for comparison of medians between placebo and rAMH groups

Table 3 Serum concentration for human AMH, human estradiol, and murine FSH in the two mice groups, placebo and rAMH, during the three time, points of the experiment

Variable	Time	Placebo group Median (Q1, Q3)	rAMH group Median (Q1, Q3)	p value[a]
AMH	Ovariectomy/pump	8.351 (8.275, 8.447)	6.988 (5.664, 7.212)	ns
	Xenotransplant	5.319 (3.424, 6.839)	3.770 (2.427, 5.740)	ns
	Euthanasia/explant	0.693 (0.670, 0.755)	2.414 (1.763, 2.450)	0.029
	p value[b]	0.050	0.011	
FSH	Ovariectomy/pump	1.05 (0.74, 1.29)	0.82 (0.63, 0.98)	ns
	Xenotransplant	2.42 (2.00, 4.80)	3.64 (3.48, 4.30)	ns
	Euthanasia/explant	5.20 (4.65, 5.45)	2.90 (2.09, 6.19)	ns
	p value[b]	0.026	0.043	
Estradiol	Ovariectomy/pump	443.4 (441.3, 583.6)	457.1 (431.4, 545.5)	ns
	Xenotransplant	305.0 (247.8, 380.0)	462.2 (461.9, 467.0)	0.048
	Euthanasia/explant	39.2 (37.0, 57.1)	141.1 (136.8, 168.4)	ns
	p value[b]	ns	ns	

[a] Mood's test for comparison of medians between placebo and rAMH groups

[b] Mood's test for comparison of medians across the three time points

cross-reaction between human and murine estradiol. Estradiol serum levels at time 7 days (xenotransplant) were not different from the ones measured at time 0 in both groups, while they sharply decreased at time 14 days, as shown in Fig. 3. In the rAMH group, estradiol levels at time 7 days were significantly higher than in the placebo group ($p = 0.048$; Table 3 and Fig. 3); however, the decrement incline from day 7 through day 14 was similar in the two groups, denoting a similar elimination process. Ovarian cortex estradiol production showed to be minimal at time 14 days in both, placebo and rAMH, groups. Serum concentrations of FSH, reported in Table 3, displayed the physiologic feedback to estradiol levels, being low at time 0, and progressively increasing at times 7, and

14 days, when estradiol levels were at their lowest. The changes displayed by FSH serum concentrations across the three time points were significantly different in both treatment groups, as shown in Fig. 3.

Real-time RT-PCR test results

The medians of the tissue markers' expression by the ovarian cortex specimens soon after warming, and in the placebo pump and rAMH pump groups, are reported in Table 4. Considering the post-thaw markers' expression as the baseline, in the placebo pump group, all markers except for AMH-R2, FSH-R, and NANOG appeared to be increased. On the
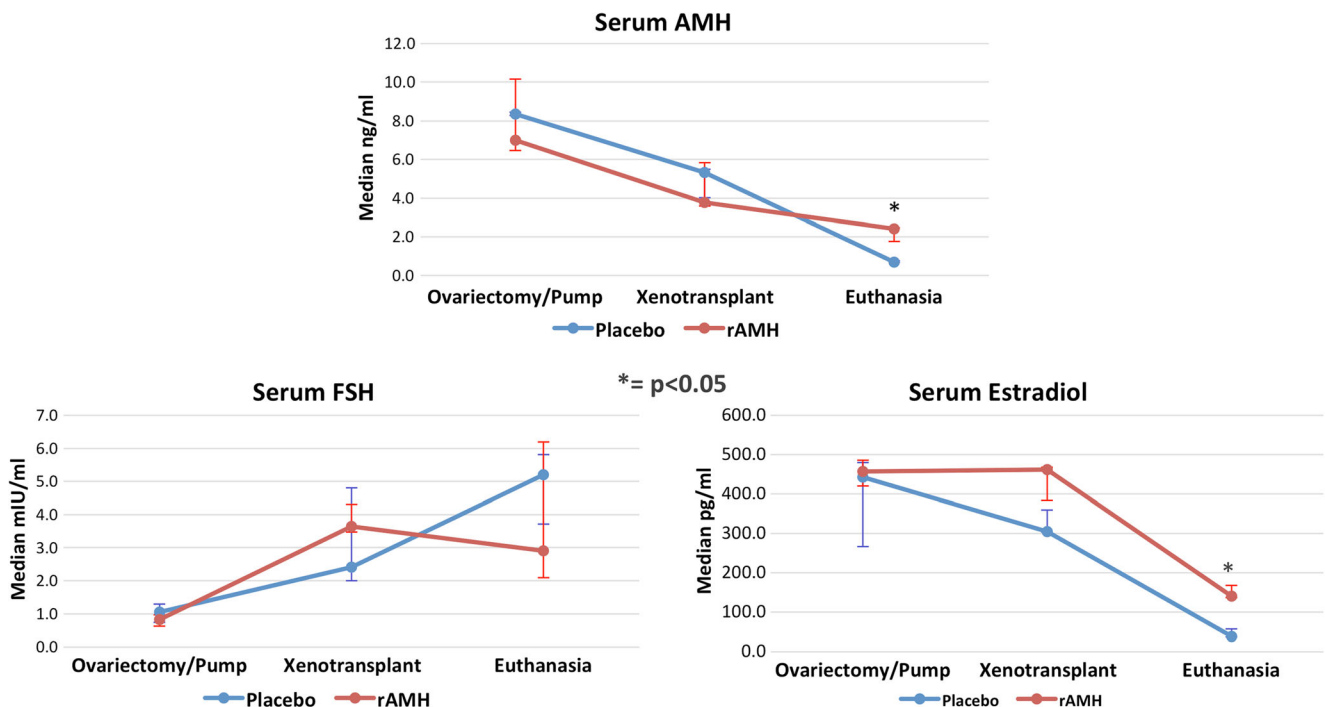

Fig. 3 Graphic representation of serum AMH, FSH, and estradiol medians with whiskers representing Q1 and Q3. Significance ($p < 0.05$) between placebo and rAMH pump groups is indicated by an asterisk

Table 4 mRNA expression of the study markers soon after specimen thawing and in the placebo and rAMH treatment groups

Marker	Post-warming Median (Q1, Q3)	Placebo pump Median (Q1, Q3)	rAMH pump Median (Q1, Q3)	p value[a]
AMH (fg/µg RNA)	0.010 (0.009, 0.010)	0.041 (0.029, 0.060)	0.0001 (0.0001, 0.0001)	0.031
AMH-R2 (fg/µg RNA)	0.020 (0.016, 0.024)	0.020 (0.017, 0.020)	0.011 (0.006, 0.021)	ns
FSH, R (fg/µg RNA)	0.165 (0.163, 0.167)	0.035 (0.031, 0.046)	0.139 (0.108, 0.154)	0.030
VEGF (fg/µg RNA)	0.012 (0.012, 0.013)	0.492 (0.442, 0.541)	0.003 (0.002, 0.004)	ns
GDF9 (fg/µg RNA)	0.012 (0.010, 0.013)	0.035 (0.033, 0.050)	0.009 (0.007, 0.010)	0.018
Oct, 4 (fg/µg RNA)	0.300 (0.242, 0.359)	2.172 (1.792, 2.413)	0.310 (0.280, 0.339)	0.018
Sox2 (pg/µg RNA)	0.005 (0.004, 0.006)	0.143 (0.108, 0.219)	0.027 (0.021, 0.033)	0.030
NANOG (fg/µg RNA)	0.057 (0.057, 0.057)	0.030 (0.024, 0.036)	0.109 (0.096, 0.121)	0.018

[a] Mood's test for comparison of medians across the three groups

other hand, in the rAMH group, all markers' expression resembled the post-thaw values, except for AMH and VEGF, which were further decreased.

Figure 4 is a graphic representation of the stemness markers' mRNA results together with the oocyte activation marker, GDF9, and the vascularization promoter, VEGF. While VEGF expression changes were not significant, the other markers' expressions were significantly decreased ($p = 0.018$ for GDF9, $p = 0.018$ for Oct4, $p = 0.030$ for Sox2), or increased ($p = 0.018$ for NANOG) in the rAMH group, where they became similar to the post-thaw expression values for all markers except for NANOG. In fact, NANOG expression further increased in the rAMH group.

Figure 5 shows the immunohistochemical staining for Ki67 and TUNEL. Counting the stained cell nuclei, there appears to be a lower cell replication and depressed apoptosis in the rAMH, compared to the placebo group. The pictures are

shown at low magnification to accentuate the tissue concentration of the stained nuclei.

Discussion

The vitrification-warming process caused a non-significant decrease in PDFs, and xenotransplantation further decreased their number. Xenotransplantation did not adversely affect the nude mice, where the transplanted tissue developed a single hilum with arterial and venous vessels that originated from the underlying muscle in all cases within 7 days. Administration of rAMH in the peri-transplant period prevented follicular activation to PRF and SEF, and post-transplant premature depletion, but did not preserve the primordial follicle number. Serum concentration of AMH, FSH, and estradiol reflected the physiologic response to ovariectomy and subsequent
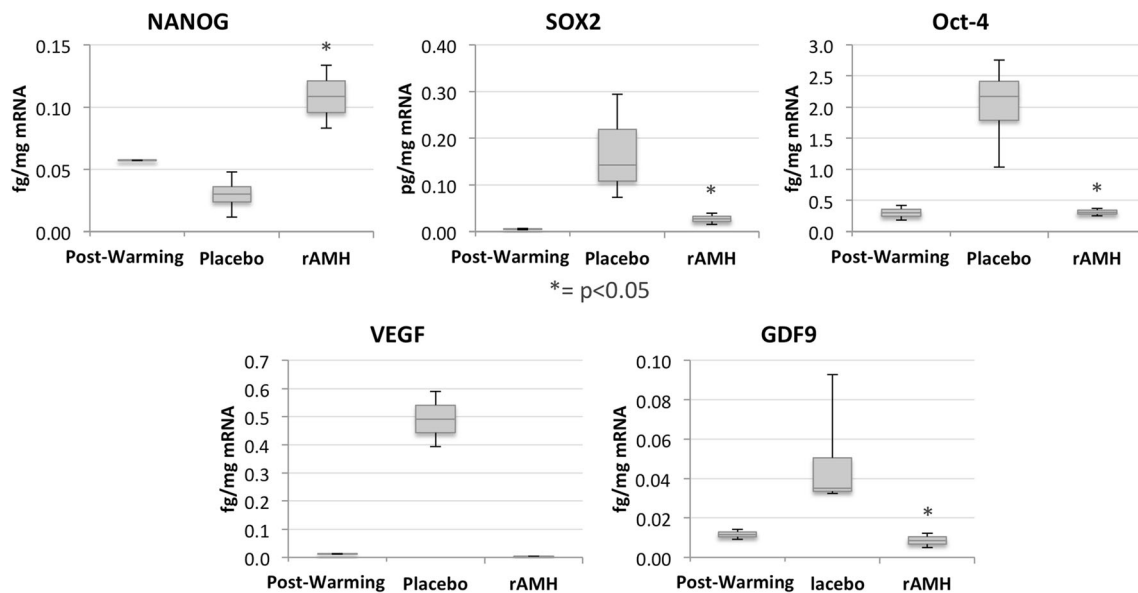

Fig. 4 **a** Box and whisker plots of ovarian cortex marker expressions in the post-thaw (pre-transplant), placebo, and rAMH groups at time of explant, on day 14 of the experiment. Significance ($p < 0.05$) is indicated by an asterisk

Fig. 5 Ki67 and TUNEL immunohistochemical staining of ovarian cortex tissue in the placebo (above) and rAMH pump (below) groups. Where positive, the cell nuclei are stained purple for Ki67 and brown for TUNEL. Follicles are indicated by black arrows
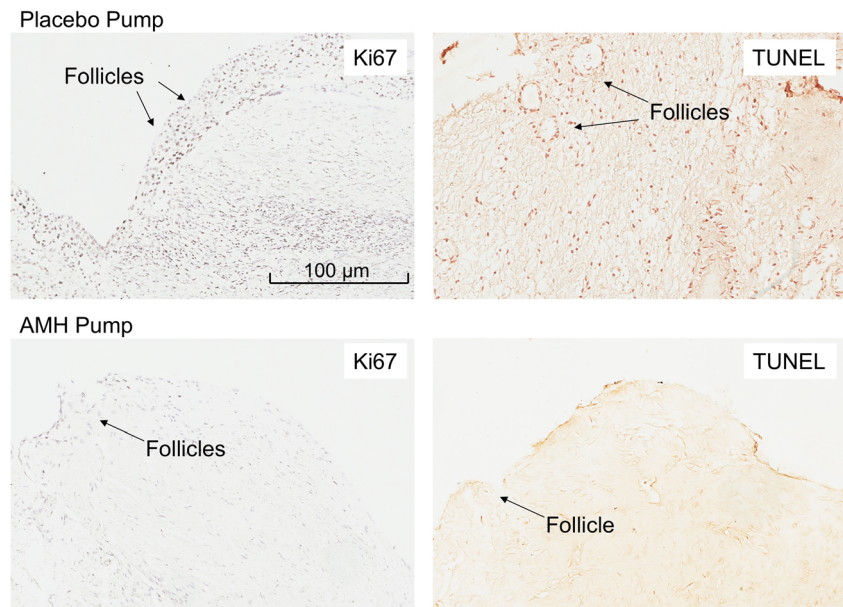
return to ovarian function in both placebo and rAMH groups. Despite some assay cross-reaction, these results testify towards a prompt return to function of the ovarian cortex shortly after transplant and re-instatement of the pituitary feedback. In the ovarian cortex, all transcription markers, except for NANOG, showed an increased expression in the placebo pump group but were not different from the post-thaw values in the rAMH group. Recombinant AMH showed the ability to protect the ovarian cortex endocrine function, as well as the expression of transcription factors in vivo, confirming the regulatory role of AMH on ovarian tissue regenerative potential.

The development of a hylum and its blood vessels, rather than scattered feeding vessels, shows that an isolated fragment of ovarian cortex can reform a structurally similar, and fully functional, ovary just a week after xenotransplant. In fact, the cortex can re-organize to fulfill its endocrine function even when deprived of its principal vascular architecture in the ovarian medullaris. AMH serum levels decreased after ovariectomy in both placebo and rAMH groups (Fig. 3). At time of euthanasia, the rAMH group showed a significantly higher serum AMH than the placebo group, which represented the pump-delivered rAMH. Despite the establishment of vasculature to the transplanted ovarian cortex, the onset of AMH production was not sufficient to be perceivable. In fact, despite some follicle development, there was a paucity of secondary follicles (only in the placebo group), and no tertiary follicles, in the pre-pubertal cortex. The fact that we were able to measure AMH at time 0 showed a cross-reaction between human and mouse AMH assays. The noted decline in AMH serum concentrations from ovariectomy to xenotranplant indicates an expected decline of AMH, similar to what was observed in the human, where AMH decline was found to follow first-order kinetics with a $t_{1/2}$ of 26.6 ± 0.8 h [24]. Since the

decrement of serum AMH was similar in the placebo and rAMH groups, we can safely imply that the decrement for human AMH in the mouse is similar to its decrement of 5.2% per day in the human. At xenotransplant, the rAMH group showed higher serum AMH than the placebo group, most probably resulting from the exogenous rAMH administration. However, AMH serum levels at time of euthanasia were increased in both groups, with different meanings: in the placebo group, the increased levels were due to endogenous production by the transplanted ovarian cortex (as confirmed by the PCR results), while in the rAMH group, they were a combination of endogenous production and exogenous administration. Despite assay cross-reaction, our results were reliable in showing rAMH-inhibited AMH production by the xenotransplanted tissue. Serum estradiol measurements reflected the physiologic response to ovariectomy; however, they showed a different profile than expected, as levels declined even after xenotransplant. This could be explained by the lack of post-transplant return to function for up to six menstrual cycles, as substantiated by human studies. In addition, because the ovarian cortex was explanted from a premenarcheal girl, the estradiol production was very limited, in view of the scant presence of secondary, and absence of tertiary, follicles and the scarce FSH stimulation by the murine pituitary. There is no report on the half-life of estradiol in the mouse; however, our results reflect the estradiol half-life in the human, which was found to be about 36 h after transdermal administration [25]. In the rAMH group, we observed a slower estradiol elimination than in the placebo group up to 14 days after ovariectomy. We do not have a good explanation for this phenomenon and future studies are underway to confirm this finding. Serum concentrations of FSH displayed the physiologic feedback to estradiol levels. However,

considering the absolute values, at time 14 days, the FSH concentration was not as high as in menopausal mice, where it can reach values greater than 15 mIU/mL [23]. This could be the result of a short time lapse between ovariectomy and euthanasia, and further research could elucidate this finding.

At tissue level, rAMH seemed to inhibit expression of all the markers evaluated, with the exception of FSH-R and NANOG, which were instead increased. Tissue AMH showed a significantly decreased expression in the rAMH pump group, providing a reason for the lower serum AMH in this group at time of euthanasia. AMH receptor expression did not change across the three groups; however, FSH-R expression significantly decreased in the placebo group, while rAMH administration caused an FSH-R expression not different from the post-warming tissue. We did not notice the previously reported decrease in FSH-R in in vivo as well as in in vitro studies [26, 27], including our previous in vitro study, where FSH-R was significantly decreased in rAMH-treated human ovarian cortex specimens compared to uncultured and untreated specimens [18]. However, the lack of tertiary follicles in our ovarian cortex specimens can explain this lack of response. In addition, the previous studies utilized higher single-solution AMH doses, rather than a continuous infusion of lower AMH doses. Nonetheless, showing a preservation of FSH-R expression in the rAMH group, our results confirm the AMH role in maintaining control of ovarian follicle development.

VEGF tissue expression in the rAMH group was similar to the post-thaw group and was lower than in the placebo group, even though the difference was non-significant. These findings unexpectedly diverged from our previous study [19], where we noticed an upregulation of VEGF in vitro expression in fresh and vitrified/warmed ovarian cortex. We are unsure how to interpret the current results; however, Fisher et al. [28] had a similar outcome when culturing intact primate follicles in the presence of recombinant FSH and found that non-growing follicles were not producing VEGF measured in the culture medium with ELISA methodology. Could our results be due to the prepubertal ovarian cortex tissue quiescence? Or could they be due to rAMH inhibition of VEGF in vivo, with the consequent hypovascularization causing ovarian cortex tissue hypofunction? We believe the pre-pubertal tissue quiescence better explains the results, as the ovarian cortex vascular pedicles were similarly developed in the two groups, providing similar oxygenation to the transplanted ovarian cortex fragments.

The oocyte function marker GDF9 and the stemness marker Oct4 and SOX2 tissue expressions showed levels similar to the post-warming ones, while NANOG's showed upregulation, when rAMH was administered. These markers' profiles were similar to the ones found in our previous in vitro study

[19]. In fact, in in vitro fresh, or vitrified/warmed, human ovarian cortex tissue, the absence of AMH caused upregulation of all the markers. The addition of rAMH for 48 h caused a decreased magnitude in tissue expression of all markers, which trended towards the baseline fresh, or post-warming, ones. With NANOG instead, rAMH administration caused an increased tissue expression. With Oct-4, and its promoter Sox2, normally promoting pluripotency, and NANOG acting to establish embryonic stem cells identity, our results corroborate the hypothesis that AMH regulates ovarian cortex stemness potential. We do not have a good explanation for opposite effects in different stemness markers, though, and further research is needed.

The H&E and immunohistochemical staining for Ki67, associated with cellular proliferation, and TUNEL, a marker of apoptosis, findings confirm the real-time RT-PCR findings of ovarian cortex quiescence in the presence of rAMH and activation in its absence. Our results confirm the findings by Kong et al. [29], where AMH treatment significantly decreased follicle apoptosis in mice autotransplanted with vitrified/warmed ovaries. In addition, a similar inhibitory effect of rAMH on cellular growth and function was previously observed on melanoma cells [8], in granulosa cells [30], and in our group's previous experiment, in which we demonstrated a decreased hormonal production and a decreased sensitivity to pituitary hormones of ovarian cortex tissue [18]. The fact that rAMH at the levels delivered by the pump entirely blocks any primordial follicle recruitment, and also likely negatively impacts any growing follicles that were in the ovarian cortex, is a remarkable finding. This level of maintaining primordial follicles in a dormant state has extremely important clinical implications, such as for prevention of follicular depletion at the time of ovarian cortex transplant, or for prevention of age-related follicular depletion. Further studies are under way to find appropriate rAMH doses.

In conclusion, our study provides insight into the in vivo effects of AMH on human pre-pubertal ovarian cortex. Exposure to rAMH did not preserve primordial follicle loss from vitrification-warming and after tissue transplant; however, it inhibited ovarian cortex activation/apoptosis after transplant, thus protecting it until vascularization of the transplant is established and its own AMH tissue production is initiated. Premature massive activation of primordial follicles would result in early apoptosis and depletion of the follicular reservoir and early exhaustion of the transplanted cortex's function. Our results provide evidence of the advantage of administering exogenous AMH at the time of pre-pubertal ovarian cortex transplant in an effort to protect the follicles from pre-activation and premature depletion.

References

1. Donnez J, Dolmans MM, Diaz C, Pellicer A. Ovarian cortex transplantation: time to move on from experimental studies to open clinical application. Fertil Steril. 2015;104:1097–8. https://doi.org/10.1016/j.fertnstert.2015.08.005.

2. Jadoul P, Dolmans MM, Donnez J. Fertility preservation in girls during childhood: is it feasible, efficient and safe and to whom should it be proposed? Hum Reprod Update. 2010;16:617–30.

3. Childhood cancer survival statistics 1973–2014. http://seer.cancer.gov. Released 4/4/2017. Accessed August 1, 2017.

4. Green DM, Kawashima T, Stovall M, Leisenring W, Sklar CA, Mertens AC, et al. Fertility of female survivors of childhood cancer: a report from the childhood cancer survivor study. J Clin Oncol. 2009;27:2677–85. https://doi.org/10.1200/JCO.2008.20.1541.

5. Corkum KS, Laronda MM, Rowell EE. A review of reported surgical techniques in fertility preservation for prepubertal and adolescent females facing a fertility threatening diagnosis or treatment. Am J Surg. 2017;214:695–700. https://doi.org/10.1016/j.amjsurg.2017.06.013.

6. Liu J, Van der Elst J, Van den Broecke R, Dhont M. Early massive follicle loss and apoptosis in heterotopically grafted newborn mouse ovaries. Hum Reprod. 2002;17:605–11.

7. Gook DA, Edgar DH. Cryopreservation of the human female gamete: current and future issues. Hum Reprod. 1999;14:2938–40.

8. Van Eyck AS, Bouzin C, Feron O, Romeu L, Van Langendonckt A, Donnez J, et al. Both host and graft vessels contribute to revascularization of xenografted human ovarian tissue in a murine model. Fertil Steril. 2010;93:1676–85.

9. Gavish Z, Spector I, Peer G, Schlatt S, Wistuba J, Roness H, et al. Follicle activation is a significant and immediate cause of follicle loss after ovarian tissue transplantation. J Assist Reprod Genet. 2017 Nov 3;35:61–9. https://doi.org/10.1007/s10815-017-1079-z.

10. Gook DA, McCully BA, Edgar DH, McBain JC. Development of antral follicles in human cryopreserved ovarian tissue following xenografting. Hum Reprod. 2001;16:417–22.

11. Flaws JA, Abbud R, Mann RJ, Nilson JH, Hirshfield AN. Chronically elevated luteinizing hormone depletes primordial follicles in the mouse ovary. Biol Reprod. 1997;57:1233–7.

12. Maltaris T, Beckmann MW, Binder H, Mueller A, Hoffmann I, Koelbl H, et al. The effect of a GnRH agonist on cryopreserved human ovarian grafts in severe combined immunodeficient mice. Reproduction. 2007;133:503–9.

13. Oktem O, Oktay K. The role of extracellular matrix and activin-A in in vitro growth and survival of murine preantral follicles. Reprod Sci. 2007;14:358–66.

14. Soleimani R, Heytens E, Oktay K. Enhancement of neoangiogenesis and follicle survival by sphingosine-1-phosphate in human ovarian tissue xenotransplants. PLoS One. 2011;6:e19475.

15. Abir R, Fisch B, Jessel S, Felz C, Ben-Haroush A, Orvieto R. Improving posttransplantation survival of human ovarian tissue by treating the host and graft. Fertil Steril. 2011;95:1205–10.

16. Yu J, Yaba A, Kasiman C, Thomson T, Johnson J. mTOR controls ovarian follicle growth by regulating granulosa cell proliferation.

17. PLoS One. 2011;6:e21415. https://doi.org/10.1371/journal.pone.0021415.

18. Zhang J, Liu W, Sun X, Kong F, Zhu Y, Lei Y, et al. Inhibition of mTOR signaling pathway delays follicle formation in mice. J Cell Physiol. 2017;232:585–95. https://doi.org/10.1002/jcp.25456.

19. Detti L, Fletcher NM, Saed GM, Peregrin-Alvarez I, Uhlmann RA. Anti-Mullerian hormone (AMH) may stall ovarian cortex function by receptor downregulation. In Press, Reprod Scien. 2017.

20. Detti L, Fletcher NM, Uhlmann RA, Saed GM. Recombinant anti-Mullerian hormone (AMH) regulates ovarian cortex's stemness potential in fresh and vitrified/thawed ovarian cortex, Under revision. Syst Biol Reprod Med. 2017.

21. Kano M, Sosulski AE, Zhang L, Saatcioglu HD, Wang D, Nagykery N, et al. AMH/MIS as a contraceptive that protects the ovarian reserve during chemotherapy. Proc Natl Acad Sci U S A. 2017;28(114):E1688–97. https://doi.org/10.1073/pnas.1620729114.

22. Parry RL, Chin TW, Epstein J, Hudson PL, Powell DM, Donahoe PK. Recombinant human mullerian inhibiting substance inhibits human ocular melanoma cell lines in vitro and in vivo. Cancer Res. 1992;52:1182–6.

23. Bullwinkel J, Baron-Lühr B, Lüdemann A, Wohlenberg C, Gerdes J, Scholzen T. Ki-67 protein is associated with ribosomal RNA transcription in quiescent and proliferating cells. J Cell Physiol. 2006;206:624–35.

24. Detti L, Uhlmann RA, Lu M, Zhang J, Diamond MP, Saed GM, et al. Serum markers of ovarian reserve and ovarian histology in adult mice treated with cyclophosphamide in pre-pubertal age. J Assist Reprod Genet. 2013;30:1421–9.

25. Griesinger G, Dafopoulos K, Buendgen N, Cascorbi I, Georgoulias P, Zavos A, et al. Elimination half-life of anti-Müllerian hormone. J Clin Endocrinol Metab. 2012;97:2160–3. https://doi.org/10.1210/jc.2012-1070.

26. Naunton M, Al Hadithy AFY, Brouwers JRBJ, Archer DF. Estradiol gel. Menopause. 2006;13:517–27. https://doi.org/10.1097/01.gme.0000191881.52175.8c.

27. Pellatt L, Rice S, Dilaver N, Heshri A, Galea R, Brincat M, et al. Anti-Müllerian hormone reduces follicle sensitivity to follicle-stimulating hormone in human granulosa cells. Fertil Steril. 2011;96:1246–1251.e1.

28. Hayes E, Kushnir V, Mia X, Biswas A, Prizant H, Gleicher N, et al. Intracellular mechanism of anti-Mullerian hormone (AMH) in regulation of follicular development. Mol Cell Endocrinol. 2016;433:56–65.

29. Fisher TE, Molskness TA, Villeda A, Zelinski MB, Stouffer RL, Xu J. Vascular endothelial growth factor and angiopoietin production by primate follicles during culture is a function of growth rate, gonadotrophin exposure and oxygen milieu. Hum Reprod. 2013;28:3263–70.

30. Kong HS, Kim SK, Lee J, Youm HW, Lee JR, Suh CS, et al. Effect of exogenous anti-Müllerian hormone treatment on cryopreserved and transplanted mouse ovaries. Reprod Sci. 2016;23:51–60. https://doi.org/10.1177/1933719115594021.

31. Di Clemente N, Goxe B, Remy JJ, et al. Inhibitory effect of AMH upon aromatase activity and LH receptors of granulosa cells of rat and porcine immature ovaries. Endocrine. 1994;2:553–8.